Methylthio- and Ethanediyldithio-Substituted 1,6-Dithiapyrenes and Their Charge-Transfer Complexes: New Organic Molecular Metals

Kazuhiro Nakasuji,*[1a] Mitsuru Sasaki,[1a] Tomoyuki Kotani,[1a] Ichiro Murata,*[1a] Toshiaki Enoki,[1b] Kenichi Imaeda,[1b] Hiroo Inokuchi,[1b] Atsushi Kawamoto,[1c] and Jiro Tanaka[1c]

Contribution from the Department of Chemistry, Faculty of Science, Osaka University, Toyonaka, Osaka 560, Japan, the Institute for Molecular Science, Okazaki 444, Japan, and the Department of Chemistry, Faculty of Science, Nagoya University, Chikusa-ku, Nagoya 464, Japan. *Received February 23, 1987*

Abstract: The synthesis and physical properties of 2,7-bis(methylthio)-1,6-dithiapyrene (MTDTPY) and 2,3:7,8-bis(ethanediyldithio)-1,6-dithiapyrene (ETDTPY) and their charge-transfer complexes are reported. MTDTPY was prepared from 1,6-dithiapyrene. ETDTPY was prepared from naphthalene-1,5-dithiol in four steps. These two new donors showed reversible two-stage redox behavior with potentials comparable to that of tetrathiafulvalene. MTDTPY produced two crystalline phases of 1:1 TCNQ complexes, the α-form (monoclinic, $P2_1/c$) and the β-form (triclinic, $P\bar{1}$), which consist of mixed stacks and uniform segregated stacks of donors and acceptors, respectively. The β-form contained short S···S contacts between adjacent donor columns (3.48 and 3.57 Å). The single-crystal conductivity of the β-form was metallic (σ_{rt} = 110 S cm^{-1}, T_c = 110 K), while that of the α-form was semiconductive ($\sigma_{rt} = 3.4 \times 10^{-6}$ S cm^{-1}). MTDTPY–chloranil crystallized in uniform segregated stacks of donors and acceptors (triclinic, $P\bar{1}$). Relatively short interstack S···S contacts were also observed (3.60 and 3.67 Å). The single-crystal conductivity was metallic (σ_{rt} = 140 S cm^{-1}, T_c = 240 K). MTDTPY–bromanil also showed metallic conductivity (σ_{rt} = 230 S cm^{-1}, T_c = 125 K). The long needle crystals of MTDTPY–$I_{2.2}$ and ETDTPY–$I_{2.3}$ showed semiconducting behavior with relatively high conductivities, 13 and 42 S cm^{-1}, respectively.

I. Introduction

The remarkable scientific processes in the realization of organic metals and superconductors based on tetrathiafulvalene (TTF) type donors have brought about a rich and new area of chemistry and physics.[2] We can draw two molecular design strategies for new donors to explore highly conducting organic solids: (1) construction of new multistage redox type donors with relatively low oxidation potentials and (2) chemical modifications on the donors to introduce interstack interactions in the solid state. The advent of such new donors might contribute to the further development of this science. As a first step, we have recently synthesized the new donors 3,10-dithiaperylene (DTPR, **1**)[3] and 1,6-dithiapyrene (DTPY, **2**),[3,4] which are termed peri-condensed Weitz-type donors.

In order to introduce multidimensionality through variations in interstack coupling, two types of modifications on the TTF skeleton have been successfully explored. The first is the replacement of sulfur atoms by selenium or tellurium atoms.[5] The second is introduction of alkylthio substituents to increase the number of chalcogen sites responsible for interstack interactions.[6,7]

Chart I

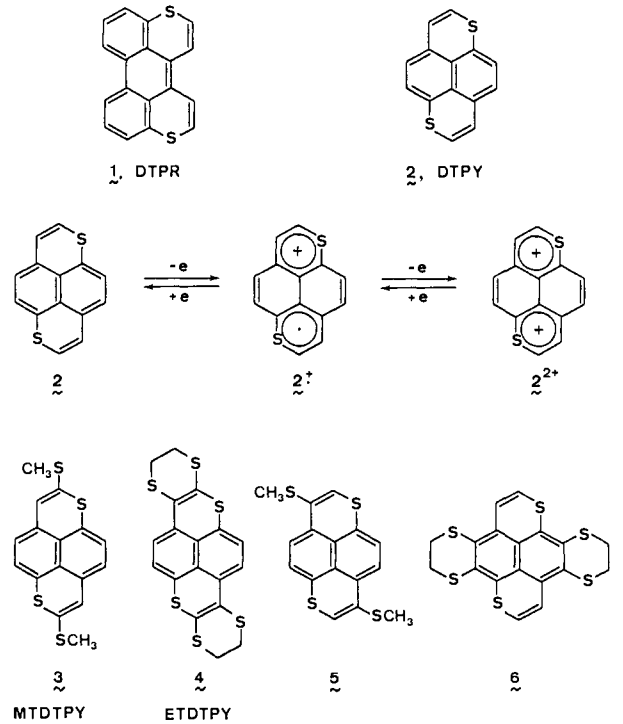

Adopting the second one, we decided to introduce methylthio groups (*MT-type modification*) or ethanediyldithio groups (*ET-*

(1) (a) Osaka University. (b) Institute for Molecular Science. (c) Nagoya University.

(2) For general reviews, see: (a) Perlstein, J. H. *Angew. Chem., Int. Ed. Engl.* **1977**, *16*, 519. (b) Torrance, J. B. *Acc. Chem. Res.* **1979**, *12*, 79. (c) Bechgaard, K.; Jerome, D. *Sci. Am.* **1982**, *247*, 52. (d) Wudl, F. *Acc. Chem. Res.* **1984**, *17*, 227. (e) Williams, J. M.; Beno, M. A.; Wang, H. H.; Leung, P. C. W.; Emge, T. J.; Geiser, U.; Carlson, K. D. *Acc. Chem. Res.* **1985**, *18*, 261. (f) Cowan, D. O.; Wiygul, F. M. *Chem. Eng. News* **1986**, July 21, 28.

(3) Nakasuji, K.; Kubota, H.; Kotani, T.; Murata, I.; Saito, G.; Enoki, T.; Imaeda, K.; Inokuchi, H.; Honda, M.; Katayama, C.; Tanaka, J. *J. Am. Chem. Soc.* **1986**, *108*, 3460.

(4) (a) Thorup, N.; Rindorf, G.; Jacobsen, C. S.; Bechgaard, K.; Johannsen, I.; Mortensen, K. *Mol. Cryst. Liq. Cryst.* **1985**, *120*, 349. (b) Bechgaard, K. *Mol. Cryst. Liq. Cryst.* **1985**, *125*, 81. (c) Tilak, B. D. *Proc. Indian Acad. Sci., Sect. A* **1951**, *33A*, 71.

(5) For some examples, see: (a) Engler, E. M.; Patel, V. V.; *J. Am. Chem. Soc.* **1974**, *96*, 7376. (b) Bechgaard, K.; Cowan, D. O.; Bloch, A. N. *J. Chem. Soc., Chem. Commun.* **1974**, 937. (c) Bloch, A. N.; Cowan, D. O.; Bechgaard, K.; Pyle, R. E.; Banks, R. H. *Phys. Rev. Lett.* **1975**, *34*, 1561. (d) Bechgaard, K.; Carneiro, K.; Rasmussen, F. B.; Olsen, M.; Rindorf, G.; Jacobsen, C. S.; Pedersen, H. J.; Scott, J. C. *J. Am. Chem. Soc.* **1981**, *103*, 2440. (e) Wudl, F.; Aharon-Shalom, E. *J. Am. Chem. Soc.* **1982**, *104*, 1154.

(6) For some examples, see: (a) Mizuno, M.; Garito, A. F.; Cava, M. P. *J. Chem. Soc., Chem. Commun.* **1978**, 18. (b) Saito, G.; Enoki, T.; Toriumi, K.; Inokuchi, H. *Solid State Commun.* **1982**, *42*, 557. (c) Parkin, S. S. P.; Engler, E. M.; Schumaker, R. R.; Lagier, R.; Lee, V. Y.; Scott, J. C.; Greene, R. L. *Phys. Rev. Lett.* **1983**, *50*, 270. (d) Yagubskii, E. B.; Schegolev, I. F.; Laukhin, V. N.; Kononovich, P. A.; Karatsovnik, M. W.; Zvarykina, A. V.; Buravov, L. I. *JETP Lett. (Engl. Transl.)* **1984**, *39*, 12. (e) Wang, H. H.; Beno, M. A.; Geiser, U.; Firestone, M. A.; Webb, K. S.; Nunez, L.; Crabtree, G. W.; Carlson, K. D.; Williams, J. M.; Azevedo, L. J.; Kwak, J. F.; Schirber, J. E. *Inorg. Chem.* **1985**, *24*, 2465.

0002-7863/87/1509-6970$01.50/0

Scheme I[a]

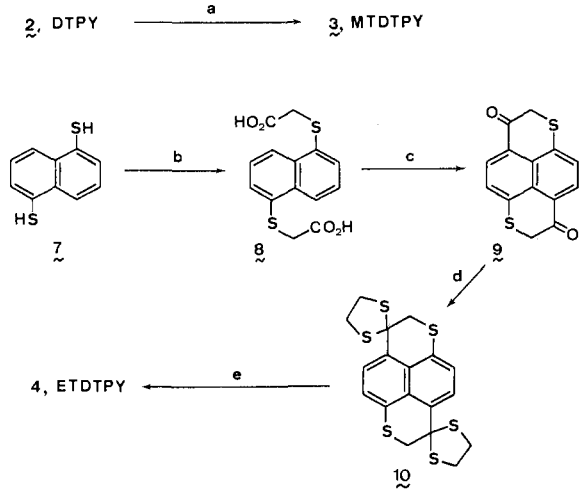

[a] (a) *n*-BuLi, THF; H_3CSSCH_3. (b) KOH, $ClCH_2CO_2H$, EtOH–H_2O. (c) $SOCl_2$; $AlCl_3$, CH_2Cl_2. (d) $HSCH_2CH_2SH$, $BF_3{\cdot}Et_2O$, CH_2Cl_2. (e) NCS, CH_2Cl_2.

Table I. Oxidation Potentials (V vs. SCE)

	2[a]	3[a]	4[b]	TTF[a]	BEDT–TTF[c]
E_1^{ox}	0.36	0.34	0.48	0.34	0.54
E_2^{ox}	0.75	0.64	0.83	0.71	0.83
ΔE	0.39	0.30	0.35	0.37	0.29

[a] CH_3CN/Et_4NClO_4. [b] $PhCN/n\text{-}Bu_4NClO_4$. [c] $CH_2Cl_2/n\text{-}Bu_4NClO_4$.

type modification) on the DTPY skeleton. We now report the synthesis and physical properties of 2,7-bis(methylthio)-1,6-dithiapyrene (MTDTPY, **3**) and 2,3:7,8-bis(ethanediyldithio)-1,6-dithiapyrene (ETDTPY, **4**), and their charge-transfer (CT) complexes.

II. Results and Discussion

A. Synthesis and Physical Properties. There exist many possible isomers of MTDTPY and ETDTPY, for example **3** and **5** for MTDTPY and **4** and **6** for ETDTPY. Although **5** and **6** also occupy an important position in study on the relationship between component molecules and solid-state properties of their CT complexes, we selected **3** and **4** as our initial targets because of their ready availability.

MTDTPY (**3**) was prepared by treatment of **2**[3] with *n*-BuLi followed by dimethyl disulfide in 78% yield. The dihydrodithiin moieties of ETDTPY (**4**) were constructed from ethylene dithioacetal (**10**) by a one-step procedure.[8] Thus, reaction of naphthalene-1,5-dithiol (**7**) with chloroacetic acid in aqueous ethanolic potassium hydroxide gave diacid (**8**) (98%), which was treated with thionyl chloride and then aluminum chloride to afford diketone **9** (42%). Thioacetalization of **9** with ethanedithiol and boron trifluoride etherate produced dithioacetal **10** (92%), which could be converted to the desired ETDTPY (**4**) by treatment with *N*-chlorosuccinimide in 9% yield. Although the yield of the final step is low, a rather short-step synthesis could provide a sufficient amount of **4** for preliminary studies of solid-state properties.

These two new donors, **3** and **4**, showed reversible two-stage redox behavior with relatively low oxidation potentials comparable to that of TTF (Table I). Although almost no effect on the potential was observed by MT-type modification on DTPY, ET-type modification resulted in a positive shift for the potential of DTPY as in the case of TTF. The alkylthio modifications on DTPY caused a slight bathochromic shift and hyperchromic effect

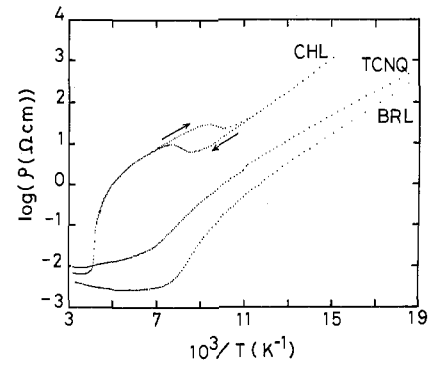

Figure 1. Temperature dependence of the resistivities for MTDTPY complexes with TCNQ, CHL, and BRL.

to the longest wavelength absorption of DTPY.

Charge-transfer complexes derived from **3** and **4** were prepared by using organic and inorganic acceptors. MTDTPY produced two crystalline (α- and β-forms, respectively) phases of 1:1 TCNQ complexes. The difference of the redox potentials between MTDTPY and TCNQ ($\Delta E^{\circ\prime} = +0.16$ V) meets the requirement of the incomplete CT proposed for various TTF–TCNQ type complexes.[9] The degree of CT (Z) determined by the IR procedure[10] is 0.36 for the α-form and 0.61 for the β-form. The Z values evaluated from the bond length ratio procedure using TCNQ geometries[11] show 0.31 and 0.71 for the α- and β-forms, respectively. Thus, the β-form exhibits higher ionicity than the α-form and incomplete charge transfer between MTDTPY and TCNQ. The electronic spectrum of the β-form shows a very low energy absorption band at near 3000 cm^{-1}, which might be assigned to an intrastack CT transition in a segregated TCNQ stack.[3,12] On the other hand, the α-form possesses no such low-energy absorption. Actually, an X-ray crystal structure analysis indicates that the β-form consists of uniform segregated stacks of donors and acceptors, while the α-form contains stacks of alternating donor and acceptor molecules (see section B). The single-crystal conductivity of the β-form is found to be metallic ($\sigma_{rt} = 110$ S cm^{-1}). Though the conductivity decreases steeply around 150 K (Figure 1), the thermopower and ESR measurements give the result that metal–insulator (M–I) transition takes place at 110 K.[13] The α-form shows a simple semiconductive behavior with $\sigma_{rt} = 3.7 \times 10^{-6}$ S cm^{-1} and $E_a = 0.26$ eV. The weaker donor ETDTPY gave a neutral 1:1 TCNQ complex.

MTDTPY gave highly conducting 1:1 complexes with *p*-benzoquinone type acceptors, fluoranil (FLL), chloranil (CHL), bromanil (BRL), and 2,3-dichloro-5,6-dicyanobenzoquinone (DDQ). In spite of fairly high conductivity with $\sigma_{rt} = 18$ S cm^{-1}, MTDTPY–FLL is a semiconductor with $E_a = 0.13$ eV. MTDTPY–CHL and MTDTPY–BRL reveal metallic conductions with $\sigma = 140$ and 230 S cm^{-1}, respectively (Figure 1). Both complexes show sharp M–I transitions, at 240 K for the CHL complex[14] and 125 K for the BRL complex. *These are the first two-chain molecular metals containing only organic π-electron systems which are not based on TTF- and TCNQ-type component molecules.*[15] MTDTPY–CHL also crystallized in uniform seg-

(7) Wu, P.; Mori, T.; Enoki, T.; Imaeda, K.; Saito, G.; Inokuchi, H. *Bull. Chem. Soc. Jpn.* **1986**, *59*, 127.
(8) Yoshino, H.; Kawazoe, Y.; Taguchi, T. *Synthesis* **1974**, 713.

(9) (a) Wheland, R. C. *J. Am. Chem. Soc.* **1976**, *98*, 3926. (b) Saito, G.; Ferraris, J. P. *Bull. Chem. Soc. Jpn.* **1980**, *53*, 2141.
(10) (a) Chappell, J. A.; Bloch, A. N.; Bryden, W. A.; Maxfield, M.; Poehler, P. O.; Cowan, D. O. *J. Am. Chem. Soc.* **1981**, *103*, 2442. (b) Girlando, A.; Pecile, C.; Painelli, A. *J. Phys. Colloq. C3, Suppl.* **1983**, *44*, 1547.
(11) Kistenmacher, T. J.; Emge, T. J.; Bloch, A. N.; Cowan, D. O. *Acta Crystallogr., Sect B: Struct. Crystallogr. Cryst. Chem.* **1982**, *B38*, 1193.
(12) (a) Torrance, J. B.; Scott, B. A.; Kaufman, F. B. *Solid State Commun.* **1975**, *17*, 1369. (b) Tanaka, J.; Tanaka, M.; Kawai, T.; Takabe, T.; Maki, O. *Bull. Chem. Soc. Jpn.* **1976**, *49*, 2358. (c) Nakasuji, K.; Nakatsuka, M.; Yamochi, H.; Murata, I.; Harada, S.; Kasai, N.; Yamamura, K.; Tanaka, J.; Saito, G.; Enoki, T.; Inokuchi, H. *Bull. Chem. Soc. Jpn.* **1986**, *59*, 207.
(13) Imaeda, K.; Enoki, T.; Mori, T.; Inokuchi, H.; Nakasuji, K.; Sasaki, M.; Murata, I., unpublished result.
(14) As for MTDTPY–CHL, a hysteresis of the resistivity suggests the presence of a first-order phase transition around 110 K.

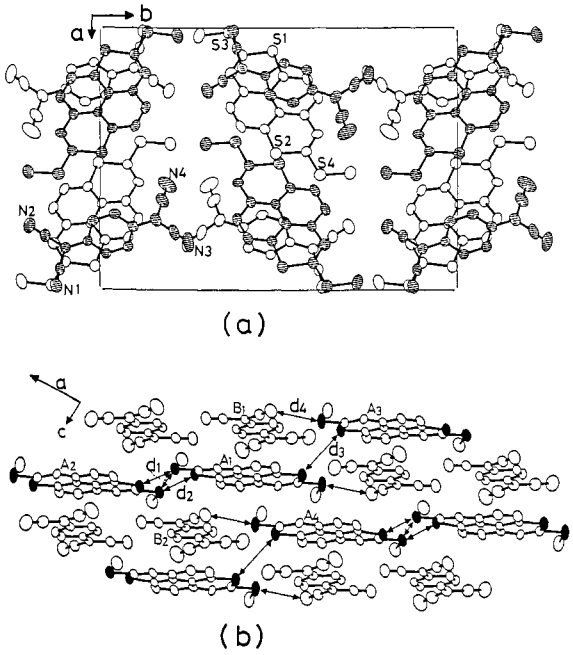

Figure 2. (a) Crystal structure of α-MTDTPY–TCNQ viewed along the c axis. (b) View of the donor and acceptor sheet in α-MTDTPY–TCNQ. Some distances: d_1 = 3.66, d_2 = 3.82, d_3 = 3.93, d_4 = 3.66 Å.

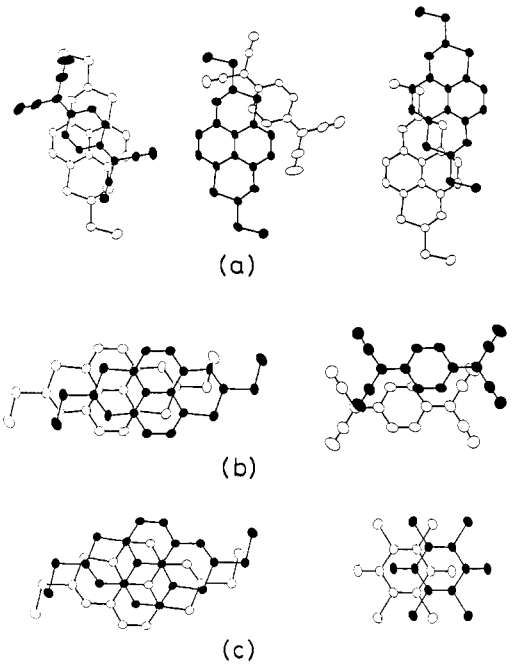

Figure 3. Molecular overlap modes: (a) α-MTDTPY–TCNQ; (b) β-MTDTPY–TCNQ; (c) MTDTPY–CHL.

regated stacks of donors and acceptors (see section B). Room-temperature conductivities of MTDTPY–DDQ are 6.3×10^{-2} S cm^{-1} (compressed pellet).

Like DTPY, both donors, **3** and **4**, gave no crystalline salts with inorganic counter ions such as BF_4 and ClO_4. However, in sharp contrast to DTPY, the two new donors easily form single crystals of the iodine complexes, MTDTPY–$I_{2.2}$ and ETDTPY–$I_{2.3}$, as long needles with metallic luster which showed semiconducting behavior

(15) For the highly conducting two-chain organic conductor containing chloranil see: (a) Torrance, J. B.; Mayerle, J. J.; Lee, V. Y.; Bechgaard, K. *J. Am. Chem. Soc.* **1979**, *101*, 4747. (b) Mayerle, J. J.; Torrance, J. B.; Crowley, J. I. *Acta Crystallogr., Sect. B: Struct. Crystallogr. Cryst. Chem.* **1979**, *B35*, 2988. (c) Mayerle, J. J.; Torrance, J. B. *Acta Crystallogr., Sect. B: Struct. Crystallogr. Cryst. Chem.* **1981**, *B37*, 2030. (d) Torrance, J. B.; Mayerle, J. J.; Lee, V. Y.; Bozio, R.; Pecile, C. *Solid State Commun.* **1981**, *38*, 1165.

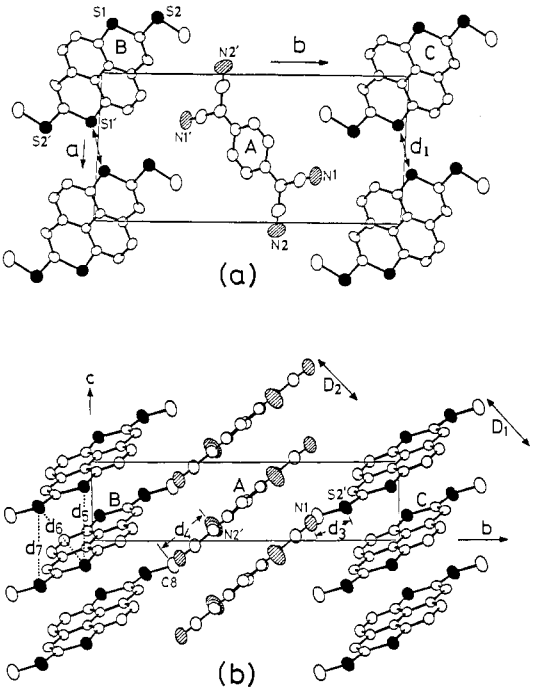

Figure 4. Crystal structures of β-MTDTPY–TCNQ viewed along (a) the c axis and (b) the a axis. Some distances: d_1 = 3.57, d_3 = 3.50, d_4 = 3.28, d_5 = 4.37, d_6 = 4.02, d_7 = 4.37, D_1 = 3.48, D_2 = 3.27 Å. For d_2, see text.

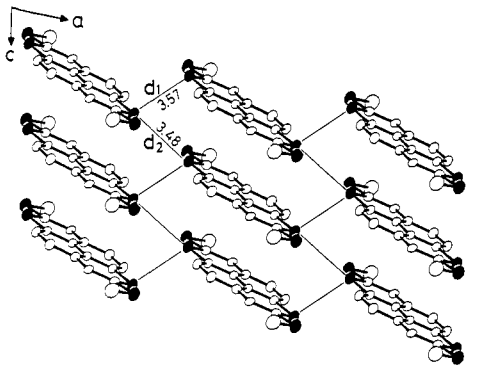

Figure 5. View of the sheet-like network of the donor molecules in β-MTDTPY–TCNQ.

with relatively high conductivities, 13 and 42 S cm^{-1}, respectively.

B. Crystal Structures. As can be seen from the unit cell view along the c axis (Figure 2a), the donor and acceptor molecules in α-MTDTPY–TCNQ stack alternately along the c axis. There exist weak donor–donor overlaps, which connect the mixed stacks into sheet-like networks (Figure 2b). The three types of overlap modes of donor–acceptor and donor–donor pairs are shown in Figure 3a. We found no intermolecular contact less than the van der Waals sum.

Unlike α-MTDTPY–TCNQ, the donor and acceptor molecules in β-MTDTPY–TCNQ are arranged in uniform, segregated stacks along the c axis. The unit cell views along the c and a axes are shown in Figure 4. The two component molecules lie on inversion centers. The interplanar distances (D_1 and D_2) are 3.48 and 3.27 Å in the donor and acceptor stacks, respectively. There are no short intrastack S···S distances (d_5, d_6, and d_7 in Figure 4b). In sharp contrast, the shorter interstack S···S contacts less than the van der Waals sum (3.70 Å) are found between sulfur atoms in the DTPY skeleton: d_1 [S1(x, y, z)···S1($-1-x, -y, 1-z$)] = 3.57 Å and d_2 [S1(x, y, z)···S1($-1-x, -y, -z$)] = 3.48 Å. Thus, on the basis of the crystal structure we expect a sheet-like two-dimensional network of the donors as shown in Figure 5. On the other hand, substituent sulfur atoms show no short interstack S···S distances less than 4 Å. The interstack distances, S···N (d_3) and N···CH_3 (d_4), are 3.50 and 3.28 Å, respectively. The overlap

Table II. Crystal Data

	α-MTDYPY-TCNQ	β-MTDTPY-TCNQ	MTDTPY-CHL
formula	$C_{28}H_{16}N_4S_4$	$C_{28}H_{16}N_4S_4$	$C_{22}H_{12}Cl_4O_2S_4$
formula wt	536.73	536.73	578.41
cryst system	monoclinic	triclinic	triclinic
space group	$P2_1/c$	$P\bar{1}$	$P\bar{1}$
a, Å	15.0829 (24)	8.2858 (29)	14.585 (2)
b, Å	20.5411 (25)	16.9568 (48)	16.957 (1)
c, Å	7.9483 (11)	4.3703 (29)	3.757 (1)
α, deg		90.118 (38)	94.91 (2)
β, deg	99.023 (12)	103.479 (43)	90.68 (2)
γ, deg		92.800 (27)	144.24 (1)
V, Å^3	2432.05 (59)	596.35 (49)	535.7 (2)
Z	4	1	1
d_{obsd}, g/cm^3	1.46	1.50	1.79
d_{calcd}, g/cm^3	1.460	1.495	1.792
cryst size, mm	0.3 × 0.15 × 0.07	0.4 × 0.05 × 0.02	0.5 × 0.1 × 0.05
no. of unique reflections	3437	1864	1680
R	0.056	0.067	0.048

Table III. Fractional Atomic Coordinates of Non-Hydrogen Atoms with Estimated Standard Deviations in Parentheses for α-MTDTPY-TCNQ

atom	x	y	z
S(1)	0.08907 (6)	0.48603 (3)	0.18062 (10)
S(2)	0.48125 (6)	0.49544 (3)	0.74977 (13)
S(3)	0.01571 (6)	0.36389 (3)	0.05429 (10)
S(4)	0.56211 (6)	0.61682 (5)	0.85386 (14)
N(1)	0.98599 (22)	−0.12403 (15)	0.95513 (41)
N(2)	0.75855 (23)	−0.19613 (15)	0.59646 (44)
N(3)	0.81840 (29)	0.25149 (16)	0.79320 (53)
N(4)	0.60063 (28)	0.19135 (23)	0.38582 (56)
C(1)	0.10374 (22)	0.40192 (15)	0.18924 (38)
C(2)	0.17349 (23)	0.37080 (16)	0.28830 (41)
C(3)	0.24386 (20)	0.40549 (15)	0.40071 (38)
C(4)	0.30728 (23)	0.36922 (15)	0.50733 (44)
C(5)	0.37805 (23)	0.39824 (15)	0.61340 (46)
C(6)	0.38861 (20)	0.46514 (15)	0.61400 (38)
C(7)	0.47389 (20)	0.57907 (15)	0.72091 (41)
C(8)	0.40806 (23)	0.60978 (15)	0.60840 (47)
C(9)	0.33442 (20)	0.57462 (14)	0.50835 (38)
C(10)	0.26909 (23)	0.61140 (15)	0.40643 (41)
C(11)	0.19700 (23)	0.58198 (15)	0.30586 (41)
C(12)	0.18665 (19)	0.51528 (15)	0.30466 (37)
C(13)	0.25207 (20)	0.47512 (14)	0.40361 (37)
C(14)	0.32534 (19)	0.50553 (14)	0.50794 (37)
C(15)	0.02908 (35)	0.28006 (20)	0.11300 (63)
C(16)	0.55496 (32)	0.70000 (19)	0.78968 (69)
C(17)	0.81693 (19)	−0.03419 (14)	0.70978 (38)
C(18)	0.74030 (23)	−0.01908 (16)	0.58402 (43)
C(19)	0.71407 (22)	0.04289 (16)	0.55147 (43)
C(20)	0.76101 (20)	0.09568 (15)	0.64298 (38)
C(21)	0.83765 (22)	0.08091 (15)	0.76772 (40)
C(22)	0.86468 (20)	0.01880 (15)	0.79901 (38)
C(23)	0.84360 (20)	−0.09748 (15)	0.74307 (38)
C(24)	0.92251 (23)	−0.11297 (15)	0.86149 (41)
C(25)	0.79625 (23)	−0.15242 (15)	0.66133 (44)
C(26)	0.73427 (25)	0.16018 (16)	0.61407 (44)
C(27)	0.78086 (29)	0.21163 (18)	0.71077 (53)
C(28)	0.65970 (29)	0.17749 (19)	0.48818 (53)

modes in the MTDTPY stacks and the TCNQ stacks are shown in Figure 3b. The relative arrangement found in the TCNQ stacks is unusual and shows no bond-over-ring type overlap.[16]

MTDTPY–CHL also crystallized in uniform, segregated stacks of donors and acceptors, as can be seen from the unit cell views along the c and b axes (Figure 6). The two component molecules lie on inversion centers. The interplanar spacings in the donor (D_1) and the acceptor stacks (D_2) are 3.47 and 3.22 Å, respectively. The intrastack S···S distances in MTDTPY–CHL (Figure 6b)

(16) Emge, J. J.; Bryden, W. A.; Wiygul, F. M.; Cowan, D. O.; Kistenmacher, T. J. *J. Chem. Phys.* **1982**, *77*, 3188.

Table IV. Fractional Atomic Coordinates of Non-Hydrogen Atoms with Estimated Standard Deviations in Parentheses for β-MTDTPY-TCNQ

atom	x	y	z
S(1)	−0.33463 (10)	0.02577 (6)	0.31549 (23)
S(2)	−0.37995 (13)	0.17283 (6)	0.58209 (26)
N(1)	−0.31607 (65)	0.71342 (23)	1.22121 (117)
N(2)	0.05223 (59)	0.60123 (34)	0.81851 (147)
C(1)	−0.24662 (44)	0.11903 (20)	0.41730 (83)
C(2)	−0.09116 (46)	0.14871 (20)	0.37289 (86)
C(3)	0.00301 (44)	0.09884 (19)	0.20318 (81)
C(4)	−0.04938 (40)	0.02115 (19)	0.08394 (77)
C(5)	−0.19942 (41)	−0.01696 (20)	0.12329 (83)
C(6)	−0.24780 (44)	−0.09294 (22)	0.00671 (93)
C(7)	0.15177 (47)	0.13285 (20)	0.15501 (93)
C(8)	−0.26528 (74)	0.26467 (29)	0.68832 (147)
C(9)	−0.37488 (50)	0.55132 (20)	0.68784 (95)
C(10)	−0.54617 (53)	0.55639 (23)	0.69167 (99)
C(11)	−0.33403 (52)	0.49211 (23)	0.49016 (102)
C(12)	−0.25084 (56)	0.60377 (23)	0.86260 (104)
C(13)	−0.28871 (59)	0.66387 (23)	1.05965 (111)
C(14)	−0.08306 (63)	0.60158 (29)	0.84132 (126)

Table V. Fractional Atomic Coordinates of Non-Hydrogen Atoms with Estimated Standard Deviations in Parentheses for MTDTPY-CHL

atom	x	y	z
S(1)	0.32257 (9)	0.34963 (6)	0.19279 (23)
S(2)	0.28577 (10)	0.48131 (7)	0.51107 (25)
Cl(1)	0.46530 (10)	0.79912 (9)	0.68226 (25)
Cl(2)	0.18799 (9)	0.68937 (7)	1.04989 (25)
O(1)	0.72936 (32)	1.09090 (28)	0.65680 (90)
C(1)	0.18859 (38)	0.32471 (32)	0.33786 (87)
C(2)	0.03160 (38)	0.19923 (32)	0.32505 (90)
C(3)	−0.04352 (35)	0.07195 (31)	0.19993 (81)
C(4)	0.04035 (35)	0.06447 (31)	0.06038 (78)
C(5)	0.20540 (35)	0.18448 (31)	0.04041 (81)
C(6)	0.28443 (35)	0.17514 (32)	−0.10540 (93)
C(7)	−0.20522 (38)	−0.04965 (34)	0.21977 (93)
C(8)	0.12686 (49)	0.43003 (41)	0.64755 (123)
C(9)	0.62578 (40)	1.04962 (35)	0.81874 (99)
C(10)	0.47849 (40)	0.90557 (35)	0.85663 (93)
C(11)	0.36186 (38)	0.85940 (35)	1.02071 (96)

are shorter than those in β-MTDTPY–TCNQ. This feature results from the difference between overlap modes in the donor stacks. Thus, a smaller slippage is found for the donor–donor overlap in MTDTPY–CHL than that in β-MTDTPY–TCNQ (Figure 3b,c). The overlap mode of the chloranil stacks, C=O double bond-over-ring pattern, is similar to that of the bromanil stacks reported in TMTTF–BRL.[15c] The interstack S···S contacts are slightly shorter than the van der Waals sum: d_1 [S1(x, y, z)···S1($1-x$, $1-y$, $-z$)] = 3.67 Å and d_2 [S1(x, y, z)···S1($1-x$, $1-y$, $1-z$)] = 3.60 Å. Again, no short interstack S···S contact between substituent sulfur atoms could be observed. Since MTDTPY–CHL contains neither a TTF-type nor TCNQ-type skeleton, there are no empirical procedures to evaluate the degree of CT (Z). However, some ionic nature of the complex could be deduced from the bond length changes found in the CHL skeleton. Thus, in the molecular geometry, C=C (1.354 Å) and C=O (1.233 Å) lengths of CHL in MTDTPY–CHL are longer than those of neutral CHL[17] by 0.010 and 0.022 Å, respectively. In addition, the averaged C—C length (1.469 Å) of CHL is shorter than that of neutral CHL by 0.021 Å. Such bond length changes indicate some contribution of anionic nature in CHL. Interestingly, quite similar bond length changes are found in the *N,N,N',N'*-tetramethyl-1,4-phenylenediamine complex, TMPD–CHL,[18] for which the Z value is determined to be 0.6 from vibrational analysis.[19] Therefore, MTDTPY–CHL can be classified an

(17) Weperen, K. J.; Visser, G. J. *Acta Crystallogr., Sect. B: Struct. Crystallogr. Cryst. Chem.* **1972**, *B28*, 338.
(18) Boer, J. L.; Vos, A. *Acta Crystallogr., Sect. B: Struct. Crystallogr. Cryst. Chem.* **1968**, *B24*, 720.

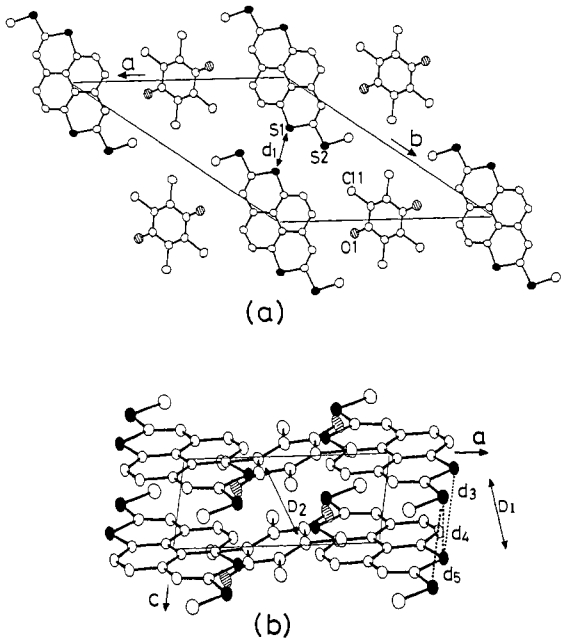

Figure 6. Crystal structures of MTDTPY-CHL viewed along (a) the c axis and (b) the b axis. Some distances: d_1 = 3.67, d_3 = 3.76, d_4 = 3.84, d_5 = 3.76, D_1 = 3.47, D_2 = 3.22. For d_2, see text.

Table VI. Intramolecular Distances (Å) for α-MTDTPY-TCNQ[a]

S(1)-C(1)	1.742 (3)	C(11)-C(12)	1.379 (5)
S(1)-C(12)	1.745 (3)	C(12)-C(13)	1.425 (4)
S(2)-C(6)	1.741 (3)	C(13)-C(14)	1.418 (4)
S(2)-C(7)	1.734 (3)	N(1)-C(24)	1.140 (4)
S(3)-C(1)	1.754 (3)	N(2)-C(25)	1.141 (5)
S(3)-C(15)	1.787 (4)	N(3)-C(27)	1.142 (5)
S(4)-C(7)	1.745 (3)	N(4)-C(28)	1.144 (6)
S(4)-C(16)	1.782 (4)	C(17)-C(18)	1.439 (4)
C(1)-C(2)	1.370 (4)	C(17)-C(22)	1.430 (4)
C(2)-C(3)	1.461 (4)	C(17)-C(23)	1.374 (4)
C(3)-C(4)	1.391 (4)	C(18)-C(19)	1.346 (5)
C(3)-C(13)	1.435 (4)	C(19)-C(20)	1.430 (5)
C(4)-C(5)	1.387 (5)	C(20)-C(21)	1.433 (4)
C(5)-C(6)	1.383 (5)	C(20)-C(26)	1.394 (5)
C(6)-C(14)	1.435 (4)	C(21)-C(22)	1.351 (4)
C(7)-C(8)	1.380 (4)	C(23)-C(24)	1.433 (4)
C(8)-C(9)	1.453 (4)	C(23)-C(25)	1.435 (4)
C(9)-C(10)	1.396 (4)	C(26)-C(27)	1.425 (5)
C(9)-C(14)	1.426 (4)	C(26)-C(28)	1.428 (5)
C(10)-C(11)	1.383 (5)		

[a] Estimated standard deviations are enclosed in parentheses.

incomplete CT and a mixed-valence complex.

The importance of MT- and ET-type modification presented in this report can be expected to be of general validity. In part to resolve detailed solid-state properties of these complexes, theoretical and physicochemical studies are under way and will be published elsewhere.

III. Experimental Section

General Methods. All melting points are uncorrected. Infrared and electronic spectra were recorded on JASCO DS-402G and Hitachi 340 spectrometers, respectively. Each IR spectrum was calibrated with indene as standard. Proton NMR spectra were measured by using Varian XL-100-15, JEOL FX-90Q, and JEOL JNM-PMX-60 spectrometers. All chemical shifts are reported in parts per million (δ) relative to internal tetramethylsilane. Mass spectra were obtained on a JEOL JMS-01SG-2 spectrometer. The cyclic voltammetries were carried out at room temperature under nitrogen with a Yanagimoto P-1100 instrument.

2,7-Bis(methylthio)-1,6-dithiapyrene (MTDTPY, 3). To a solution of **2** (721 mg, 3.00 mmol) in THF was added over 5 min 1.6 N *n*-BuLi (4.5 mL, 7.2 mmol) in hexane at −70 °C. The mixture was warmed to 10 °C over 1 h and then cooled to −70 °C. To the mixture was added dimethyl disulfide (0.64 mL, 7.2 mmol), and the resulting mixture was stirred for 45 min at −70 °C and allowed to warm to room temperature over 1.5 h. After evaporation of THF, the mixture was treated with water and extracted with benzene. The extracts were dried over magnesium sulfate and concentrated under reduced pressure. The resulting residue was purified by column chromatography on alumina (eluted with benzene) followed by recrystallization from benzene to give **3** (777 mg, 78%): orange plates, mp 149–150 °C; ^{1}H NMR (90 MHz, CS_2) δ 2.29 (6 H, s, SCH_3), 5.91 (2 H, s, H-3), 6.08 (2 H, d, J = 7.9 Hz, H-4 or -5), 6.23 (2 H, d, J = 7.9 Hz, H-5 or -4); UV λ_{max} (toluene) 415 (log ϵ 4.13), 457 nm (4.04); MS m/e (relative intensity) 332 (M^+, 100). Anal. Calcd for $C_{16}H_{12}S_4$: C, 57.79; H, 3.64; S, 38.57. Found: C, 57.90; H, 3.65; S, 38.55.

1,5-Bis((carboxymethyl)thio)naphthalene (8). To a solution of **7**[4c] (50.0 g, 0.26 mol) in ethanol (500 mL), water (900 mL), and potassium hydroxide (75.0 g, 1.34 mol) was added chloroacetic acid (75.0 g, 0.79 mol) at 0 °C, and the mixture was stirred for 5 h at room temperature. After having been cooled to 0 °C, the mixture was acidified with dilute HCl. The resulting precipitates were collected by filtration, washed with water and acetone, and dried under reduced pressure at 125 °C to give faint yellow solids of **8** (78.7 g, 98%): mp 253–254 °C (recrystallized from methanol); MS m/e (relative intensity) 308 (M^+, 32%); IR (KBr) 1700, 2200–3400 cm^{-1}. Anal. Calcd for $C_{14}H_{12}O_4S_2$: C, 54.53; H, 3.92; S, 20.79. Found: C, 54.46; H, 4.08; S, 20.20.

2,3,7,8-Tetrahydro-1,6-dithiapyrene-3,8-dione (9). A mixture of **8** (15.0 g, 0.048 mol) and $SOCl_2$ (45 mL, 0.62 mol) was heated at 85 °C for 2 h. After removal of excess $SOCl_2$ under reduced pressure, the resulting solids were dispersed in CH_2Cl_2 (1.5 L) and cooled to −50 °C. To the dispersion was added $AlCl_3$ (27 g, 0.20 mol) over 10 min. After stirring at −30 °C for 40 min, the mixture was poured onto ice. The organic layer was washed with water and dried over magnesium sulfate. Twice filtration of the solution through a short silica gel column and evaporation afforded microcrystals of **9** (5.64 g, 43%): faint green plates (recrystallization from CH_2Cl_2); mp 250 °C (dec); ^{1}H NMR (90 MHz, $CDCl_3$) δ 3.85 (4 H, s), 7.73 (2 H, d, J = 7.9 Hz), 8.16 (2 H, d, J = 7.9 Hz); MS m/e (relative intensity) 272 (M^+, 100%); IR (KBr) 1670 cm^{-1}. Anal. Calcd for $C_{14}H_8O_2S_2$: C, 61.74; H, 2.96; S, 23.55. Found: C, 61.74; H, 3.01; S, 23.37.

2,3,7,8-Tetrahydro-1,6-dithiapyrene-3,8-dione 3,8-Bis(ethylene thioacetal) (10). To a suspension of **9** (4.00 g, 14.7 mmol) and 1,2-ethanedithiol (3.7 mL, 44 mmol) in CH_2Cl_2 (200 mL) was added boron trifluoride etherate (1.5 mL, 12 mmol) over 5 min at room temperature. After 38 h of stirring, dilute aqueous NaOH was added, and the resulting precipitates were collected by filtration to give the crude solids of **10** (5.73 g, 92%): colorless plates (recrystallization from THF); mp 239 °C (dec); ^{1}H NMR (90 MHz, $CDCl_3$) δ 3.50–3.66 (8 H, m), 3.61 (4 H, s), 7.40 (2 H, d, J = 7.9 Hz), 8.20 (2 H, d, J = 7.9 Hz); MS m/e (relative intensity) 424 (M^+, 48%). Anal. Calcd for $C_{18}H_{16}S_6$: C, 50.90; H, 3.80; S, 45.30. Found: C, 50.53; H, 3.77; S, 44.41.

2,3:7,8-Bis(ethanediyldithio)-1,6-dithiapyrene (ETDTPY, 4). To a suspension of **10** (2.00 g, 4.71 mmol) in CH_2Cl_2 (2 L) was added *N*-chlorosuccinimide (140 mg, 10.5 mmol) over 5 min at 0 °C. After

Table VII. Intramolecular Distances (Å) for β-MTDTPY-TCNQ[a]

S(1)-C(1)	1.722 (4)	C(5)-C(6)	1.390 (5)
S(1)-C(5)	1.732 (4)	C(6)-C(7′)	1.380 (6)
S(2)-C(1)	1.743 (4)	N(1)-C(13)	1.160 (7)
S(2)-C(8)	1.786 (5)	N(2)-C(14)	1.149 (8)
C(1)-C(2)	1.416 (5)	C(9)-C(10)	1.430 (6)
C(2)-C(3)	1.485 (6)	C(9)-C(11)	1.426 (6)
C(3)-C(4)	1.425 (5)	C(9)-C(12)	1.405 (5)
C(3)-C(7)	1.396 (5)	C(10)-C(11′)	1.358 (5)
C(4)-C(5)	1.419 (5)	C(12)-C(13)	1.426 (7)
C(4)-C(4′)	1.434 (7)	C(12)-C(14)	1.417 (7)

[a] Estimated standard deviations are enclosed in parentheses.

Table VIII. Intramolecular Distances (Å) for MTDTPY-CHL[a]

S(1)-C(1)	1.737 (7)	C(4)-C(4′)	1.419 (10)
S(1)-C(5)	1.740 (5)	C(5)-C(6)	1.396 (9)
S(2)-C(1)	1.749 (5)	C(6)-C(7′)	1.375 (7)
S(2)-C(8)	1.796 (8)	O(1)-C(9)	1.233 (7)
C(1)-C(2)	1.359 (4)	Cl(1)-C(10)	1.719 (7)
C(2)-C(3)	1.434 (7)	Cl(2)-C(11)	1.718 (3)
C(3)-C(4)	1.429 (9)	C(9)-C(10)	1.467 (4)
C(3)-C(7)	1.399 (4)	C(9)-C(11′)	1.471 (10)
C(4)-C(5)	1.422 (4)	C(10)-C(11)	1.354 (8)

[a] Estimated standard deviations are enclosed in parentheses.

(19) Girlando, A.; Painelli, A.; Pecile, C. *Mol. Cryst. Liq. Cryst.* **1985**, *120*, 17.

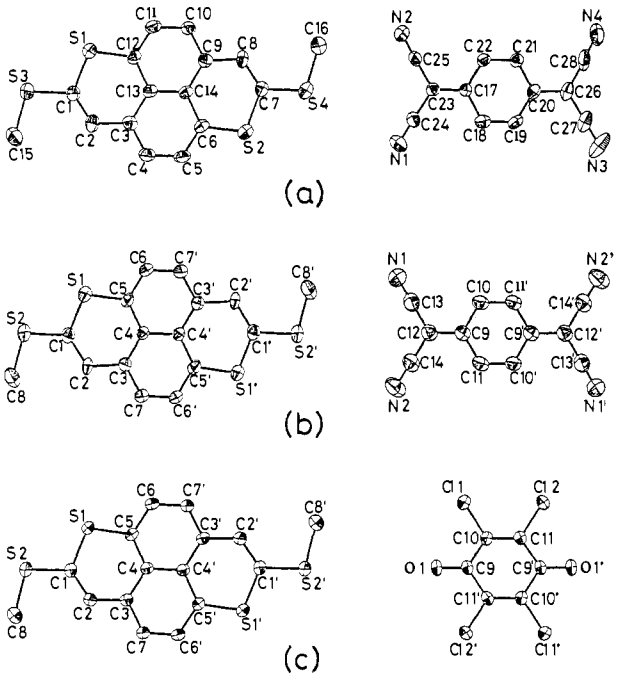

Figure 7. Atomic numbering schemes: (a) α-MTDTPY-TCNQ; (b) β-MTDTPY-TCNQ; (c) MTDTPY-CHL.

stirring for 40 h at room temperature, the mixture was washed with water, dried over magnesium sulfate, and evaporated. A benzene solution of the resulting residue was passed through an alumina column. Recrystallization from benzene to afford reddish violet plates of **4** (182 mg, 9%): mp 268–269 °C (recrystallization from benzene); UV λ_{max} (toluene) 462 (log ϵ 4.14), 427 (4.09), 321 nm (3.88); ^{1}H NMR (100 MHz, CS_2/CD_2Cl_2) δ 3.15–3.23 (8 H, m), 6.59 (2 H, d, J = 8.0 Hz), 7.13 (2 H, d, J = 8.0 Hz); MS m/e (relative intensity) 420 (M^+, 10%). Anal. Calcd for $C_{18}H_{12}S_6$: C, 51.39; H, 2.88; S, 45.73. Found: C, 51.17; H, 2.86; S, 45.71.

Preparation of the CT Complexes. Two phases of MTDTPY-TCNQ were prepared by diffusion methods using acetonitrile solutions of both components. The α-form crystals suitable for X-ray diffraction and conductivity measurement are easily obtained as black needles, prisms, and plates, though the β-form crystals are formed with much difficulty. The α-form is more lustrous than the β-form. ETDTPY-TCNQ (black needles) was prepared by mixing solutions of the two components in CH_2Cl_2. The complexes (black needles) of MTDTPY with FLL, CHL, BRL, and DDQ were obtained by mixing solutions of the donor and the acceptor in CH_2Cl_2 and by slow concentration of the solvent. MTDTPY-$I_{2.2}$ (greenish black needles) was prepared by a diffusion method using acetonitrile solutions of MTDTPY and n-Bu_4NI_3. ETDTPY-$I_{2.3}$ (black needles) was prepared by electrocrystallization using benzonitrile solutions of ETDTPY and n-Bu_4NI_3 at a constant current of ca. 1 μA.

The stoichiometries of donors and acceptors were determined by elemental analyses. MTDTPY-TCNQ (mixture of α- and β- forms). Anal. Calcd for $C_{28}H_{16}N_4S_4$: C, 62.66; H, 3.00; N, 10.44. Found: C, 62.31; H, 3.06; N, 10.28. MTDTPY-FLL. Anal. Calcd for $C_{22}H_{12}F_4O_2S_4$: C, 51.55; H, 2.36. Found: C, 51.65; H, 2.35. MTDTPY-CHL. Anal. Calcd for $C_{22}H_{12}Cl_4O_2S_4$: C, 45.68; H, 2.09. Found: C, 45.56; H, 2.13. MTDTPY-BRL. Anal. Calcd for $C_{22}H_{12}Br_4O_2S_4$: C, 34.94; H, 1.60. Found: C, 35.04; H, 1.66. MTDTPY-DDQ. Anal. Calcd for $C_{24}H_{12}Cl_2N_2O_2S_4$: C, 51.52; H, 2.16; N, 5.01. Found: C, 51.34; H, 2.17; N, 4.99. MTDTPY-$I_{2.2}$. Anal. Calcd for $C_{16}H_{12}I_{2.2}S_4$: C, 31.42; H, 1.98. Found: C, 31.29; H, 2.12. ETDTPY-TCNQ. Anal. Calcd for $C_{30}H_{16}N_4S_6$: C, 57.66; H, 2.58; N, 8.97. Found: C, 57.32; H, 2.60; N, 8.89. ETDTPY-$I_{2.3}$. Anal. Calcd for $C_{18}H_{12}I_{2.3}S_6$: C, 30.34; H, 1.70. Found: C, 30.61; H, 1.77.

Electrical Conductivity Measurements. Electrical conductivities were measured with a two-probe method for α-MTDTPY-TCNQ and a four-probe method for the other complexes. Electrical contacts were achieved with gold paste. Temperature dependences of the resistivities for three metallic complexes are shown in Figure 1.

Crystal Structure Analyses. The X-ray diffraction data were collected by using a Rigaku automated four-circle diffractometer with Cu Kα radiation monochromatized by graphite (λ(Cu Kα) = 1.5418 Å, 2θ–ω scans, $2\theta_{max}$ = 126°). The structures were solved by the Monte Carlo direct method[20] by use of the MULTAN-78[21] program system and refined on F^2 by the full-matrix least-squares method.[22] An analytical absorption correction was applied for α-MTDTPY-TCNQ. Atomic scattering factors were taken from ref 23. Anisotropic temperature factors were used for the refinement of non-H atoms. All H atoms were located from a difference Fourier map and were refined with isotropic temperature factors equivalent to that for the bonded carbon atoms. All computations were carried out at the Computation Center of Nagoya University. Crystallographic data are given in Table II. The atomic coordinates are listed in Tables III–V. Bond lengths are listed in Tables VI–VIII. The atomic numbering schemes are shown in Figure 7.

Acknowledgment. This research was supported by a Grant-in-Aid for Special Project Research (No. 6012930) and a Grant-in-Aid for Scientific Research (No. 61540370) from the Ministry of Education, Science and Culture, Japan.

(20) Furusaki, A. *Acta Crystallogr., Sect A: Found. Crystallogr.* **1979**, *A35*, 220.
(21) Main, P.; Hull, S. E.; Lessinger, L.; Germain, G.; Declercq, J. P.; Woolfson, M. M. MULTAN-78, University of York, York, England and Louvain, Belgium, 1978.
(22) Katayama, C.; Sakabe, N.; Sakabe, K. *Acta Crystallogr., Sect. A* **1972**, *A28*, S207.
(23) *International Tables for X-ray Crystallography*; Kynoch Press: Birmingham, England, 1974; Vol. IV.